J Mater Sci (2009) 44:6356–6362
DOI 10.1007/s10853-009-3876-y

Temperature-controlled assembly and morphology conversion of $CoMoO_4 \cdot 3/4H_2O$ nano-superstructured grating materials

Jing Zhao · Qing-Sheng Wu · Ming Wen

Received: 2 April 2009 / Accepted: 9 September 2009 / Published online: 25 September 2009

Abstract The regular and homogeneous single-crystal $CoMoO_4 \cdot 3/4H_2O$ nanorods, with the diameters ca. 100–300 nm and lengths ca. 8–15 μm, have been successfully prepared by a simple and facile precipitation method. Their morphology conversion from broom-like to cage-like structure has been firstly reported through controlling the reaction temperature. The broom-like microbunches were obtained at 50 °C while at 80 °C, dispersive nanorods can be prepared. As the temperature reached 90 °C, the morphology of the products converted to cage-like microspheres. SEM results show that the reaction temperature has a critical role in both the formation of the products and their morphologies. The UV–visible diffuse reflectance absorbance spectra of the products display two intense, broad absorbance bands cover almost the whole ultraviolet and visible region except for a narrow region around 450 nm, which is in the region for purple light. Based on the experimental results, a possible formation mechanism was also proposed. The synthesis strategy is simple, facile, mild, and has a good reproducibility. The as-prepared products may have potential applications in optics, catalysis, and grating materials.

J. Zhao · Q.-S. Wu (✉) · M. Wen
Department of Chemistry, Tongji University, Shanghai 200092, China
e-mail: qswu@tongji.edu.cn

M. Wen
e-mail: m_wen@tongji.edu.cn

Q.-S. Wu
Shanghai Key Laboratory of Molecular Catalysis and Innovative Materials, Fudan University, Shanghai 200433, People's Republic of China

Introduction

Nowadays, numerous researches have been focused on the metal molybdates due to their various significant properties [1–5]. Cobalt molybdate ($CoMoO_4$) is one of the most important components of industrial catalysts for the partial oxidation of hydrocarbons and precursors in the synthesis of hydrodesulphurization catalysts [6, 7]. Moreover, $CoMoO_4$ can be also applied in electroindustry and bioscience due to their structural, magnetic, electronic, and antibacterial properties [8–13].

Generally, $CoMoO_4$ can be prepared by two ways [14]. One is through the reaction between molybdenum trioxide and cobalt oxides at high temperature (ceramic method) [15]. The other is by soft chemical routes, e.g., precipitation from aqueous solutions of soluble salts of Mo and Co [16, 17], followed by calcination at temperatures 200–900 °C which are lower than that of the former method. $CoMoO_4$ may exist in several phases: the low temperature α-phase, the high temperature β-phase, the high-pressure hp-phase, and the hydrate [7]. Recently, nanomaterials with small dimensions have attracted increasing attention for their novel properties and potential applications [18, 19]. So far, a number of synthesis methodologies have been developed to fabricate and assemble nanostructure materials, however, only a few reports on preparing $CoMoO_4$ nanomaterials, for instance, Yu et al. [20] synthesized $CoMoO_4$ microrods through the hydrothermal method at 140 °C under a high pressure for 12 h. The crystalline $CoMoO_4$ nanorods with an average diameter of 10 nm were obtained in reverse micelles under hydrothermal conditions for the first time [11]. It was reported that the nanocrystalline $CoMoO_4$ powders were prepared from the complete evaporation of a polymer-based metal-complex precursor solution which was constituted by the

complexation of the metal ions and EDTA in the presence of DEA [21]. Bao et al. [22] have also synthesized ultrafine particles via a sol–gel method with citric acid as complexant, then calcined at 500 °C for 4 h. Peng et al. [23] mixed the reaction solution and stirred for 2 h, then a heat-treatment at 400 °C. However, these preparation processes need a higher temperature and/or organic additives. Additionally, some methods have a complicated process. Also, up to now, only $CoMoO_4$ nanorods and nanoparticles have been prepared, but, to the best of our knowledge, the superstructures of $CoMoO_4$, especially the conversion of those, yet have not been reported.

In this article, we develop a simple and facile precipitation method to prepare the $CoMoO_4{\cdot}3/4H_2O$ nanorods and superstructures at mild temperature under atmospheric pressure, which needs no complicated instruments, no complicated processes, no additives, and no high temperature and pressure. At the same time, nano-superstructures were self-assembled and the broom-to-cage morphology conversion of products was, for the first time, achieved through controlling the reaction temperature. The strong and comprehensive absorbance in the whole ultraviolet and visible region except for a narrow region around 450 nm indicates the products might be good grating materials for pure purple light.

Experimental procedure

Synthesis

All the reagents were of analytical grade and used without further purification. Purified water, obtained by means of a water-purification system, was used in the experiments. Take the preparation of the typical product—$CoMoO_4{\cdot}3/4H_2O$ nanorods for example, the experiment was performed as follows: cobalt nitrate solution (10 mL, 0.1 M) and sodium molybdate solution (10 mL, 0.1 M) were mixed together and stirred to form a homogeneous solution. Then the mixed solution was heated at 80 °C for 3 h in air and cooled to room-temperature naturally without stir. The purple precipitation was obtained, separated by centrifugation, and washed with purified water and absolute ethanol several times, respectively. Finally, the as-prepared products were dried under vacuum at 60 °C for further characterization. The broom-like and cage-like $CoMoO_4{\cdot}3/4H_2O$ were achieved with the same operation except for different reaction temperature and time.

Characterization

The crystal phase and purity of the products were characterized by X-ray powder diffraction (XRD, Model D/max2550VB3+/PC, Rigaku, Japan) equipped with graphite monochromatized CuKa radiation ($\lambda = 1.54056$ Å), employing a scanning rate of 0.02° s^{-1}. The operation voltage and current were maintained at 40 kV and 100 mA, respectively. The cell lattice constants of samples were calculated and corrected by MDI Jade (5.0 edition) software. The morphology and size were investigated with scanning electron microscopy (SEM, Model Philip XL30, Holland) at an accelerating voltage of 20 kV. Transmission electron microscopy (TEM), and high-resolution transmission electron microscopy (HRTEM, Model JEM-2010, JEOL, Tokyo, Japan) with fast Fourier transformation (FFT) and selected area electron diffraction (SAED) at an accelerating voltage of 200 kV. UV–visible diffuse reflectance absorbance spectra (UV-DRS) were obtained with a UV–vis spectrometer (Model BWS003, Newark, Germany). The thermal stability of the products was investigated by a simultaneous thermogravimetric and differential scanning calorimetric system (TG/DSC, Netzsch STA 409PC, Germany) with Al_2O_3 powder as the reference. Approximately 10 mg of the sample was loaded into a standard Al_2O_3 boat. The heating process was performed from 40 to 1,000 °C at heating rate of 10 °C/min, and then constant temperature for 20 min; finally, the cooling procedure was demonstrated from 1000 to 250 °C at cooling rate of 10 °C/min. All the processes were presented in a nitrogen atmosphere. Infrared spectra (4,000–400 cm^{-1}) were recorded by a Nicolet 5DX FTIR spectrometer equipped with a TGS/PE detector and a silicon beam splitter with 1 cm^{-1} resolution.

Results and discussion

The crystal structure and purity of the products were characterized by XRD. Figure 1b shows XRD pattern of $CoMoO_4{\cdot}3/4H_2O$ prepared at 80 °C for 3 h. The results can be indexed as the phase for $CoMoO_4{\cdot}3/4H_2O$, which are in agreement with the literature [8, 20]. No other peaks were observed in the pattern, showing the high purity of the sample. The $CoMoO_4{\cdot}3/4H_2O$ products were calcined at 500 °C, forming a new kind of product, the XRD pattern of which can be easily indexed to monoclinic β-$CoMoO_4$ (Fig. 1d) with $a = 10.25$ Å, $b = 9.28$ Å, $c = 7.04$ Å, $\beta = 107.12°$ (JCPDS No. 21-0868).

The thermal behavior of $CoMoO_4{\cdot}3/4H_2O$ was investigated by TG-DSC in nitrogen atmosphere at a heating rate of 10 °C min^{-1}. As shown in Fig. 2, the total weight loss is 11.7%. The TG curve shows that the weight loss increases comparatively quickly from room temperature to 350 °C and thereafter slightly changes during the rest time. There are two endothermic peaks on the DSC curve. The first one at 350 °C should be ascribed to the dehydration of

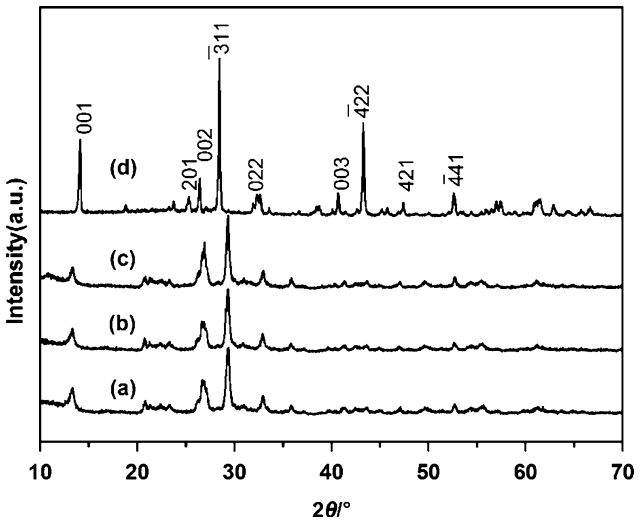

Fig. 1 XRD patterns of $CoMoO_4{\cdot}3/4H_2O$ products prepared at (*a*) 50 °C, (*b*) 80 °C, (*c*) 90 °C for 3 h, and (*d*) *β*-$CoMoO_4$ after calcination at 500 °C

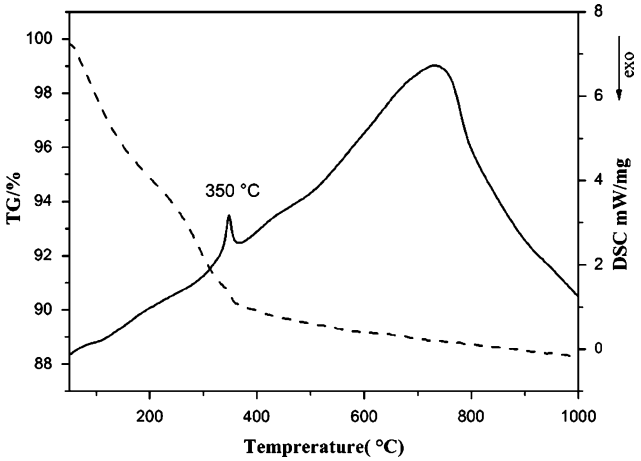

Fig. 2 TG and DSC curves of $CoMoO_4{\cdot}3/4H_2O$ products prepared at 80 °C for 3 h

$CoMoO_4{\cdot}3/4H_2O$, which is also accordance with the weight loss on the TG curve. While the second one might owing to an evident phase transition process of the $CoMoO_4$.

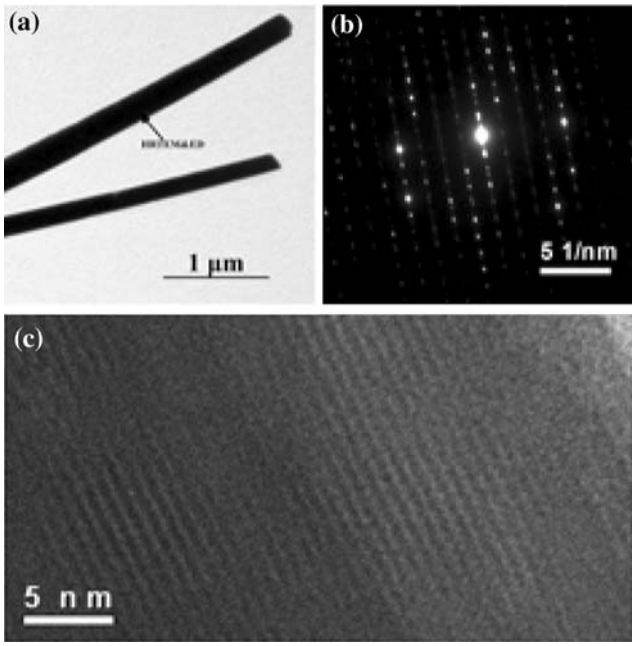

Fig. 4 **a** TEM image, **b** the ED pattern, and **c** HRTEM image of a typical $CoMoO_4{\cdot}3/4H_2O$ nanorod prepared at 80 °C for 3 h

Figure 3 shows typical SEM images of $CoMoO_4{\cdot}3/4H_2O$ products prepared at 80 °C for 3 h. It can be seen that the products consist of large-scale and homogeneous $CoMoO_4{\cdot}3/4H_2O$ nanorods. The diameters of the nanorods are ca. 100–300 nm and the lengths ca. 8–15 μm. To further investigate crystal structure and growth process of $CoMoO_4{\cdot}3/4H_2O$ nanostructures, TEM, HRTEM, and SAED were used to examine the products. Figure 4a shows a TEM image, it displays the nanorods are smooth without other particles. The HRTEM image (insert in Fig. 4c) and SAED pattern (insert in Fig. 4b) reveal the nanorods are structurally uniform without defects and dislocations. Furthermore, these nanorods exhibit a single-crystal nature.

In order to investigate the effects of the experiment conditions on the products, a series of parallel experiments were carried out, such as the reaction temperature, time, and the initial concentration. It was found that the reaction temperature had a significant influence on both the formation of products and their morphologies. When the

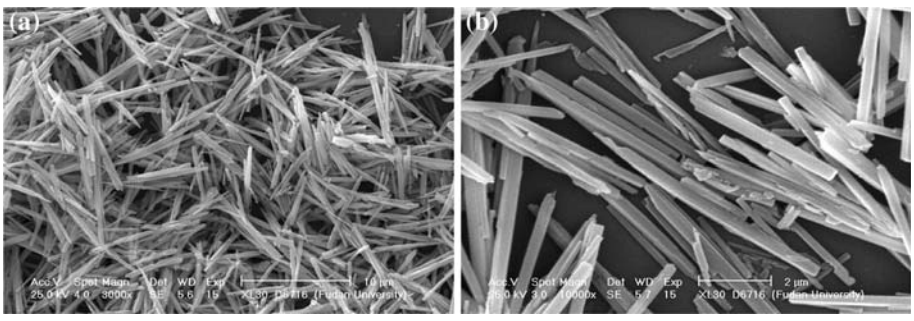

Fig. 3 Typical SEM images of $CoMoO_4{\cdot}3/4H_2O$ products prepared at (**a**, **b**) 80°C for 3 h

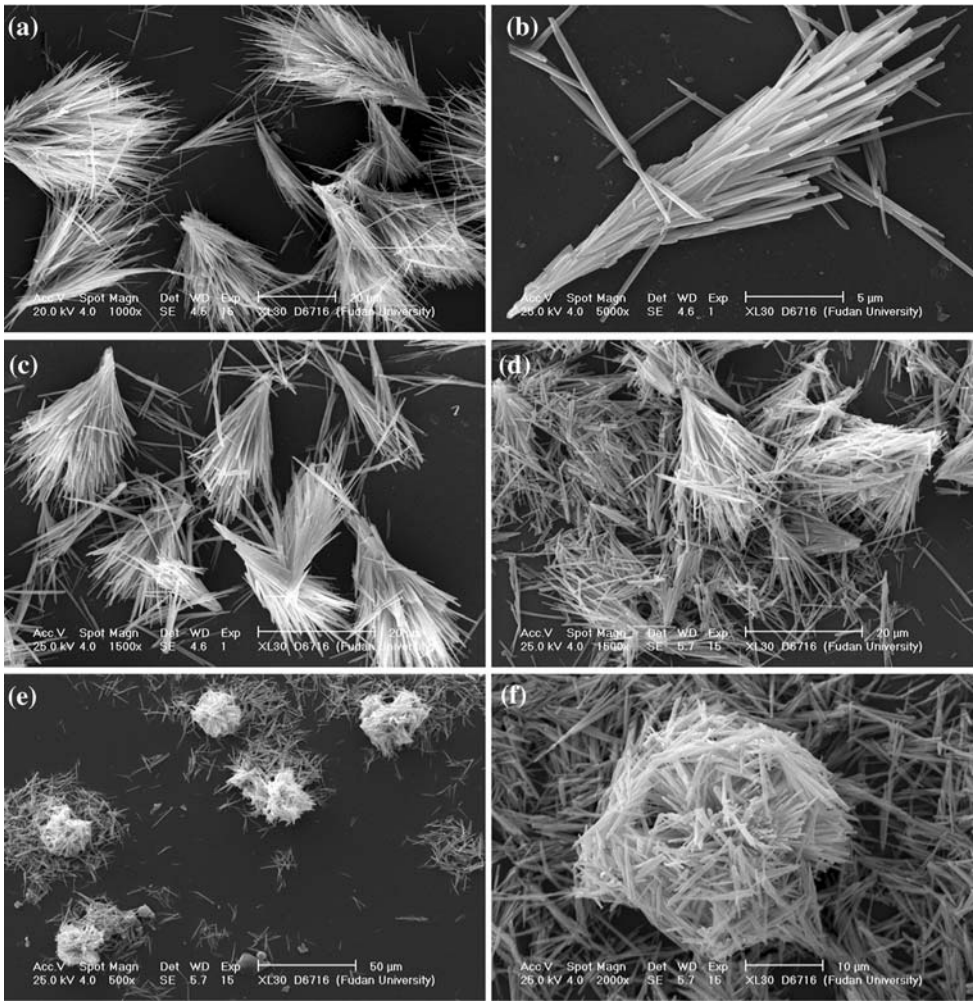

Fig. 5 Typical SEM images of $CoMoO_4 \cdot 3/4H_2O$ products prepared at: **a**, **b** 50 °C; **c** 60 °C; **d** 70 °C; **e**, **f** 90 °C for 3 h

reaction temperature was below 50 °C, no reaction occurred and only pink transparent solution was obtained. As the temperature increased up to 50 °C, small amount of the purple precipitation appeared which proved to be our aimed products (Fig. 1a). Figure 5a, b exhibit SEM images of the samples obtained at 50 °C for 3 h. $CoMoO_4$ crystal grew into broom-like microbunches, which are composed of many nanorods with the diameters around 1–2 μm and the lengths around 10–20 μm. When the reaction temperature arrived at 60 or 70 °C, besides some microbunches, some separated nanorods were clearly observed, as shown in Fig. 5c, d. We found that more and more nanorods appeared with the increase of the temperature. When the temperature increased up to 80 °C, a totally large-scale of dispersive nanorods were obtained as shown in Fig. 3a, b. When the reaction temperature kept on rising to as high as 90 or 100 °C, the products have the same structures (Fig. 1c) and the dispersive nanorods with the lengths 4–5 μm started to assemble into cage-like microspheres superstructures with diameters of ca. 30 μm as shown in Fig. 5e, f.

In addition, the reaction time also has considerable effects on the formation of the products. When the reaction time was less than 1 h at 50 °C, no products was obtained. Figure 6 shows SEM images of the growth process of broom-like self-assembled microbunches obtained at 50 °C. A lot of short tiny nanorods (Fig. 6a) appeared when the reaction time was 1 h. When the time was 2 h, there have been some nanowires (Fig. 6b). As the reaction time increased to 3 h, microbunches were achieved (Fig. 5a), however, the morphologies of the as-obtained samples almost remained the same with the rising of the reaction time (Fig. 6c, d).

The concentration-dependent experiments were carried out to monitor the initial concentration influence on the products. The reaction time kept 3 h as a constant. The molar ratio of Co/Mo remains 1. When the concentration of reactants was 0.05 M, the broom-like microbunches (Fig. 7a) were achieved when the reaction temperature was 90 °C, lower than which, however, no product was obtained. At the reactant concentration of 0.2 M, broom-like microbunches were achieved at 50 °C while the

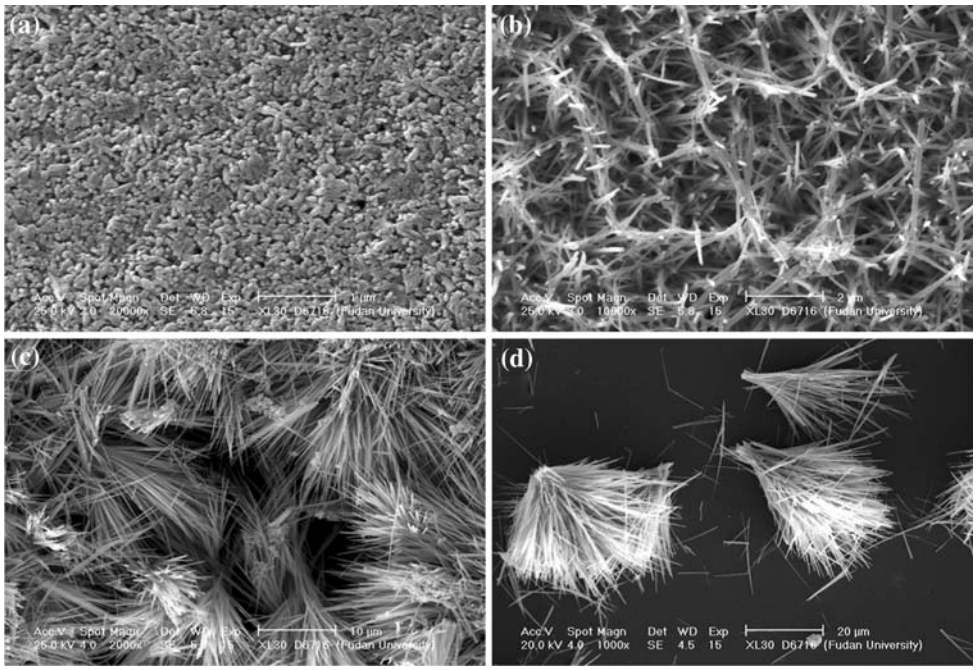

Fig. 6 Typical SEM images of $CoMoO_4 \cdot 3/4H_2O$ products prepared at 50 °C for: **a** 1 h, **b** 2 h, **c** 4 h, and **d** 6 h

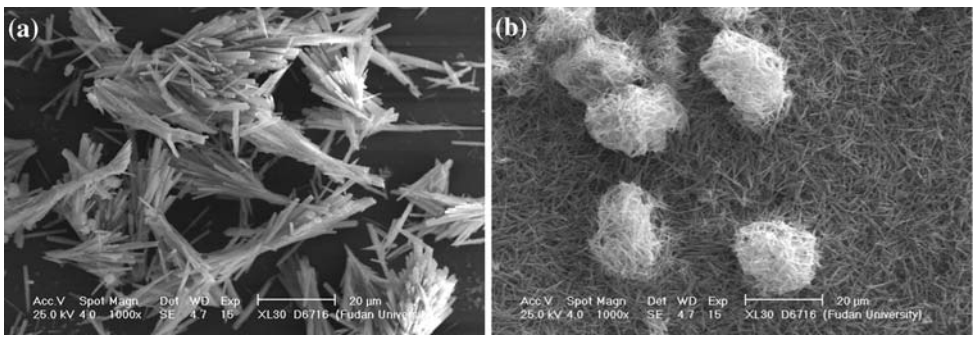

Fig. 7 Typical SEM images of $CoMoO_4 \cdot 3/4H_2O$ products prepared when the initial concentration is: **a** 0.05 M and **b** 0.3 M at 90 °C for 3 h

cage-like microspheres were achieved at 80 and 90 °C. When being 0.3 M, only cage-like microspheres (Fig. 7b) were obtained with different reaction temperature. So when the temperature is high, the initial concentration has influence on the morphologies of the products to a certain extent.

From the above results, it can be concluded that the morphologies of the $CoMoO_4 \cdot 3/4H_2O$ were influenced by reaction temperature, time, and the initial concentration, of which the first-named was dominant. All the products have no phase transformation occurring in our experiment. In addition, the yield increased dramatically with the increase of temperature, time, and concentration.

The formation process of different morphologies via temperature-controlled procedure may be described as follows (Scheme 1): the growing process of crystal includes two steps: an initial nucleating stage and growth stage. In the beginning, the mixed transparent solution became supersaturated solution when temperature rise to 50 °C, the nuclei appeared and then many of them grew up into tiny particles (Fig. 6a) which further grew into the nanowires (Fig. 6b). Extending the reaction time, one end of the nanowires tends to aggregate together, the broom-like morphology (Fig. 5a) formed [24]. As the temperature increased and the collision of cobalt cations and molybdate anions became more fiercely, assembled nuclei were getting fewer. At higher temperature, the motion of solvent molecules became fiercer. Assembled nuclei become fewer. When the temperature reached 80 °C, nuclei could hardly get together owing to fierce thermo-motion of solvent molecules and formed separated nanorods with lengths shorter than that of 50 °C. When the temperature continued to rise to 90 °C, $CoMoO_4$ molecules started to hydrolyze, generating hydroxyl radicals on the nanorod surface. Figure 8 displays the FTIR spectra of the products at 50, 80, and 90°C. Through careful analysis of the IR spectra, it is noticed that there is a slight red shift of the stretching vibration frequency of aqua hydroxyl radicals in the IR spectrum of the products at 90 °C in comparison

Scheme 1 Schematic illustration of the formation process of the $CoMoO_4 \cdot 3/4H_2O$ products

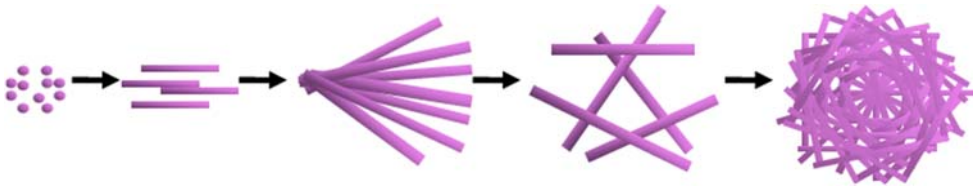

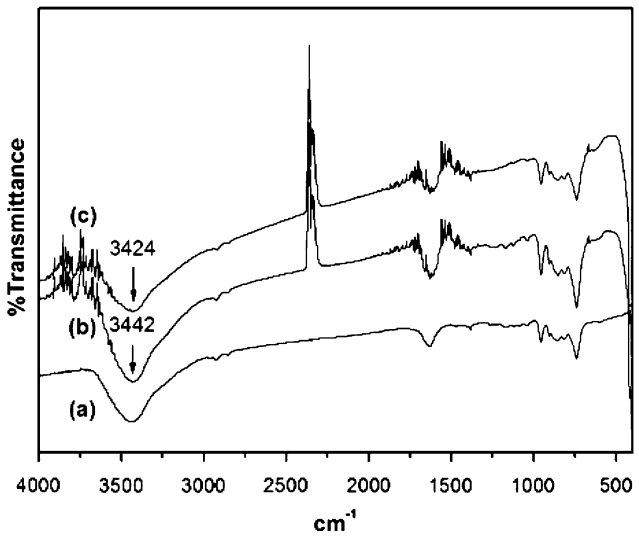

Fig. 8 FTIR spectra of $CoMoO_4 \cdot 3/4H_2O$ products prepared at (*a*) 50 °C, (*b*) 80 °C, and (*c*) 90 °C for 3 h

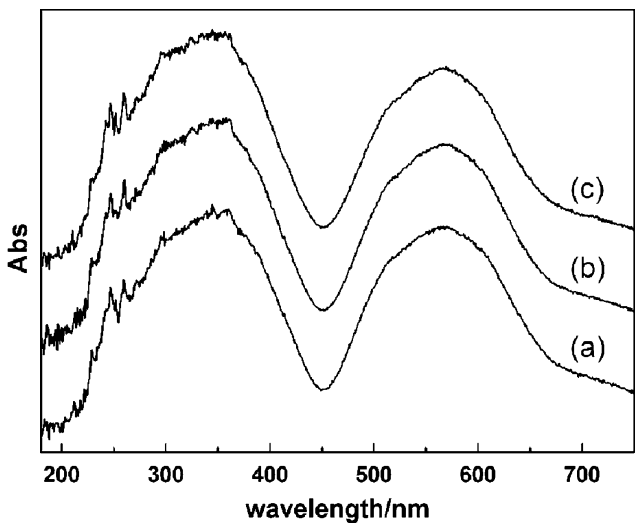

Fig. 9 UV–visible diffuse reflectance absorbance spectra of $CoMoO_4 \cdot 3/4H_2O$ products prepared at (*a*) 50 °C, (*b*) 80 °C, and (*c*) 90 °C for 3 h

with those of products at 50 and 80 °C. Therefore, hydrogen bonds were formed between the nanorods, resulting the self-assembling to form 3D cage-like structure that is propitious to stability [25–28].

The UV-DRS of $CoMoO_4$ synthesized at different temperature for 3 h are shown in Fig. 9. Each curve has two broad absorbance bands with similar intensity and width from the ultraviolet to the visible region. In the UV scope, there are obvious absorbance peaks at 357 nm, while in the visible light region, the absorbance region centered at 563 nm. The absorption of $CoMoO_4$ is usually derived from the electron transfer between the 2p HOMO of oxygen atoms and the 4d LUMO of Mo atomic [29, 30]. The absorbance of products almost cover the whole visible light range except for a narrow region around 450 nm, which is in the region of purple light. This suggests that the products can be utilized as the grating materials for pure purple light. The strong and comprehensive absorbance also indicates potential applications in fields of photosensor, photocatalysis, etc., the related investigation is under way.

Conclusions

In summary, the regular and homogeneous single-crystal $CoMoO_4 \cdot 3/4H_2O$ nano-superstructured materials have been successfully prepared through a simple and facile precipitation method. The morphology conversion through controlling the reaction temperature has been firstly reported and the possible growth mechanism in this system has been discussed. The strong and comprehensive absorbance in the whole ultraviolet and visible region except for a narrow region around 450 nm indicates the products might be good grating for pure purple light. Further research will involve investigating the relative chemical and physical properties and potential applications of the $CoMoO_4 \cdot 3/4H_2O$ nanorods. We believe that our method could be used for the preparation of other metal molybdate nanoparticles and might be applied in photocatalysis and other fields.

Acknowledgements We thank the financial support of the National Natural Science Foundation (No. 50772074) of China, the State Major Research Plan (973) of China (No. 2006CB932302), the Shanghai Key Laboratory of Molecular Catalysis and Innovative Materials (No. 2009KF04), the key program for basic research of Shanghai ST committee (No. 09JC1414100), and the Nano-Foundation of Shanghai in China (No. 0852nm01200).

References

1. Longo VM, de Figueiredo AT, Campos AB, Espinosa JWM, Hernandes AC, Taft CA, Sambrano JR, Varela JA, Longo E (2008) J Phys Chem A 112:8920
2. Wang GJ, Long XF, Zhang LZ, Wang GF (2008) J Cryst Growth 310:624
3. Ryu JH, Kim KM, Mhin SW, Park GS, Eun JW, Shim KB, Lim CS (2008) Appl Phys A: Mater Sci Process 92:407
4. Bu WB, Xu YP, Zhang N, Chen HR, Hua ZL, Shi JL (2007) Langmuir 23:9002
5. Dong FQ, Wu QS (2008) Appl Phys A: Mater Sci Process 91:161
6. Miller JE, Jackson NB, Evans L, Sault AG, Gonzales MM (1999) Catal Lett 58:147
7. Rodriguez JA, Chaturvedi S, Hanson JC, Brito JL (1999) J Phys Chem 103:770
8. Eda K, Uno Y, Nagai N, Sotani N, Whittingham MS (2005) J Solid State Chem 178:2791
9. Rodriguez JA, Chaturvedi S, Hanson JC, Albornoz A, Brito JL (1998) J Phys Chem B 102:1347
10. Ehrenberg H, Wiesmann M, Garcia-Jaca J, Weitzel H, Fuess H (1998) J Magn Magn Mater 182:152
11. Kong YM, Peng J, Xin ZF, Xue B, Dong BX, Shen FS, Li L (2007) Mater Lett 61:2109
12. Wiesmann M, Ehrenberg H, Wltschek G, Zinn P, Weitzel H, Fuess H (1995) J Magn Magn Mater 150:L1
13. Meng YY, Xiong ZX (2008) Key Eng Mater 368–372:1516
14. Calafat A, Vivas F, Brito JL (1998) Appl Catal A 172:217
15. Smith GW (1962) Acta Crystallogr 15:1054
16. Kashif I, Soliman AA, El-Bahy ZM (2008) J Alloys Compd 452:384
17. Brito JL, Barbosa AL (1997) J Catal 171:467
18. Xia YN, Yang PD, Sun YG, Wu YY, Mayers B, Gates B, Yin YD, Kim F, Yan HQ (2003) Adv Mater 15:353
19. Cui Y, Lieber CM (2001) Science 291:851
20. Ding Y, Wan Y, Min YL, Zhang W, Yu SH (2008) Inorg Chem 47:7813
21. Sen A, Pramanik P (2001) Mater Lett 50:287
22. Bao J, Bian GZ, Fu YL (1999) Chin J Catal 20:645
23. Peng C, Gao L, Yang SW, Sun J (2008) Chem Commun 43:5601
24. Silver J, Martinez-Rubio MI, Ireland TG, Fern GR, Withnall R (2001) J Phys Chem B 105:948
25. Roosen AR, Carter WC (1998) Physica A 261:232
26. Matijevic E (1993) Chem Mater 5:412
27. Sun YG, Yin YD, Mayers BB, Herricks T, Xia YN (2002) Chem Mater 14:4736
28. Caswell KK, Bender CM, Murphy CJ (2003) Nano Lett 3:667
29. Zhang Y, Holzwarth NAW, Williams RT (1998) Mater Phys 57:12738
30. Spassky DA, Ivanov SN, Kolobanov VN, Mikhailin VV, Zemskov VN, Zadneprovski BI, Potkin LI (2004) Radiat Meas 38:607